Supporting Information For

Hydrogen-Bonding Motifs and Proton-Transfer Dynamics in Electronically Excited 6-Hydroxy-2-Formylfulvene

by

Zachary N. Vealey, Lidor Foguel, and Patrick H. Vaccaro*

Department of Chemistry, Yale University
New Haven, CT 06520-8107 USA

Contents:

*Corresponding Author: Electronic Mail Address: patrick.vaccaro@yale.edu
Telephone/Fax Number: (203) 432-3975/(203) 432-6144

Section S1: Full Reference Citations.

(22) Arunan, E.; Desiraju, G. R.; Klein, R. A.; Sadlej, J.; Scheiner, S.; Alkorta, I.; Clary, D. C.; Crabtree, R. H.; Dannenberg, J. J.; Hobza, P., Kjaergaard, H. G.; Legon, A. C.; Mennucci, B.; Nesbitt, D. J., Definition of the Hydrogen Bond (IUPAC Recommendations 2011). *Pure Appl. Chem.* **2011,** *83*, 1637-1641.

(70) Frisch, M. J.; Trucks, G. W.; Schlegel, H. B.; Scuseria, G. E.; Robb, M. A.; Cheeseman, J. R.; Scalmani, G.; Barone, V.; Petersson, G. A.; Nakatsuji, H.; Li, X.; Caricato, M.; Marenich, A. V.; Bloino, J.; Janesko, B. G.; Gomperts, R.; Mennucci, B.; Hratchian, H. P.; Ortiz, J. V.; Izmaylov, A. F.; Sonnenberg, J. L.; Williams; Ding, F.; Lipparini, F.; Egidi, F.; Goings, J.; Peng, B.; Petrone, A.; Henderson, T.; Ranasinghe, D.; Zakrzewski, V. G.; Gao, J.; Rega, N.; Zheng, G.; Liang, W.; Hada, M.; Ehara, M.; Toyota, K.; Fukuda, R.; Hasegawa, J.; Ishida, M.; Nakajima, T.; Honda, Y.; Kitao, O.; Nakai, H.; Vreven, T.; Throssell, K.; Montgomery Jr., J. A.; Peralta, J. E.; Ogliaro, F.; Bearpark, M. J.; Heyd, J. J.; Brothers, E. N.; Kudin, K. N.; Staroverov, V. N.; Keith, T. A.; Kobayashi, R.; Normand, J.; Raghavachari, K.; Rendell, A. P.; Burant, J. C.; Iyengar, S. S.; Tomasi, J.; Cossi, M.; Millam, J. M.; Klene, M.; Adamo, C.; Cammi, R.; Ochterski, J. W.; Martin, R. L.; Morokuma, K.; Farkas, O.; Foresman, J. B.; Fox, D. J. *Gaussian 16, Revision A.03*, Gaussian, Inc.: Wallingford, CT, 2016.

(71) Frisch, M. J.; Trucks, G. W.; Schlegel, H. B.; Scuseria, G. E.; Robb, M. A.; Cheeseman, J. R.; Scalmani, G.; Barone, V.; Mennucci, B.; Petersson, G. A.; Nakatsuji, H.; Caricato, M.; Li, X.; Hratchian, H. P.; Izmaylov, A. F.; Bloino, J.; Zheng, G.; Sonnenberg, J. L.; Liang, W.; Hada, M.; Ehara, M.; Toyota, K.; Fukuda, R.; Hasegawa, J.; Ishida, M.; Nakajima, T.; Honda, Y.; Kitao, O.; Nakai, H.; Vreven, T.; Montgomery, J. A., Jr.; Peralta, J. E.; Ogliaro, F.; Bearpark, M.; Heyd, J. J.; Brothers, E.; Kudin, K. N.; Staroverov, V. N.; Keith, T.; Kobayashi, R.; Normand, J.; Raghavachari, K.; Rendell, A.; Burant, J. C.; Iyengar, S. S.; Tomasi, J.; Cossi, M.; Rega, N.; Millam, J. M.; Klene, M.; Knox, J. E.; Cross, J. B.; Bakken, V.; Adamo, C.; Jaramillo, J.; Gomperts, R.; Stratmann, R. E.; Yazyev, O.; Austin, A. J.; Cammi, R.; Pomelli, C.; Ochterski, J. W.; Martin, R. L.; Morokuma, K.; Zakrzewski, V. G.; Voth, G. A.; Salvador, P.; Dannenberg, J. J.; Dapprich, S.; Parandekar, P. V.; Mayhall, N. J.; Daniels, A. D.; Farkas, Ö.; Foresman, J. B.; Ortiz, J. V.; Cioslowski, J.; Fox, D. J. *Gaussian Development Version, Revision H.27*, Gaussian, Inc.: Wallingford, CT, 2012.

(72) Stanton, J. F.; Gauss, J.; Cheng, L.; Harding, M. E.; Matthews, D. A.; Szalay, P. G. *CFOUR, Coupled-Cluster Techniques for Computational Chemistry, A Quantum-Chemical Program Package (ver. 2.00b)*, 2014; with contributions from Auer, A. A.; Bartlet, R. J.; Benedikt, U.; Berger; C., Bernholdt, D. E.; Bomble, Y. J.; Christiansen, O.; Engle, F.; Faber, R.; Heckert, M.; Heun, O.; Hilgenberg, M.; Huber, C.; Jagau, T.-C.; Jonsson, D.; Jusélius, J.; Kirsch, T.; Klein, K.; Lauderdale, W. J.; Lipparini, F.; Metzroth, T.; Mück, L. A.; O'Neill, D. P.; Price, D. R.; Prochnow, E.; Puzzarini, C.; Ruud, K.; Schiffman, F.; Schwalbach, W.; Simmons, C.; Stopkowicz, S.; Tajti, A.; Vázquez, J.; Wang, F.; Watts, J. D.; including the integral packages MOLECULE (Almlöf, J.; Taylor, P. R.), PROPS (Taylor, P. R.), ABACUS (Helgaker, T.; Jensen, Aa.; Jørgensen, P.; Olsen, J.), and ECP routines by Mitin, A. V.; van Wüllen, C; see http://www.cfour.de for current version.

	ZPE-Corrected Barrier Heights ($\Delta E'_{pt}$)		
Method	**Harmonic (cm^{-1})**	**Anharmonic (cm^{-1})**	**Difference (cm^{-1})**
HF/apVDZ	1611.8	1586.4	25.4
B3LYP/apVDZ	–380.1	–383.2	3.0
M06-2X/apVDZ	–344.2	–391.8	47.6
ωB97X/apVDZ	–34.2	–20.5	–13.7
B2PLYP/apVDZ	229.8	227.5	2.3
MP2/apVDZ	–268.2	–269.1	0.9

Table S1: Anharmonic Contributions to the Proton-Transfer Barrier.

The role of anharmonic corrections in predictions of zero-point-corrected barrier heights ($\Delta E'_{pt}$) is examined for various quantum-chemical methods that implement analytical second derivatives and allow for the efficient execution of VPT2 calculations. Each wavefunction-based (HF, MP2), density functional (B3LYP, M06-2X, & ωB97X), and hybrid (B2PLYP) treatment utilized an augmented correlation-consistent basis set of double-ζ quality (aug-cc-pVDZ ≡ apVDZ). Aside from listing the values of $\Delta E'_{pt}$ deduced from matching harmonic and anharmonic force field, the differences between these quantities are tabulated so as to highlight the minimal impact that vibrational anharmonicity exerts on estimates of proton-transfer barriers.

Table S2: Predicted Spectroscopic Parameters for HFF.

The $\tilde{X}\,^1\mathrm{A}_1$ and $\tilde{A}\,^1\mathrm{B}_2$ stationary-point geometries predicted for equilibrium, transition-state, and second-order saddle-point structures of HFF were used to estimate the attendant rotational constants (A, B, C), asymmetry parameters (κ), and inertial defects (ΔI). Tabulated values, which stem from ground-state and excited-state methods deemed to be of similar theoretical accuracy, can be compared to the analogous coupled-cluster results presented in the main text.

Method	Constants	$\tilde{X}\,^1A_1$ State		$\tilde{A}\,^1B_2$ State		
		EQ	**TS(C_{2v})**	**EQ**	**TS(C_2)**	**2SP(C_{2v})**
HF/apVTZ & CIS/apVTZ	$A(\mathrm{cm}^{-1}\times10^2)$	8.985	9.917	8.777	9.645	9.575
	$B(\mathrm{cm}^{-1}\times10^2)$	5.508	5.485	5.422	5.464	5.455
	$C(\mathrm{cm}^{-1}\times10^2)$	3.415	3.532	3.352	3.523	3.475
	κ	–0.248	–0.388	–0.237	–0.366	–0.351
	$\Delta I(\mathrm{amu}\cdot\mathrm{Å}^2)$	0	0	0	–4.81	0
B3LYP/apVTZ & TD-B3LYP/apVTZ	$A(\mathrm{cm}^{-1}\times10^2)$	9.359	9.720	8.916	9.556	9.383
	$B(\mathrm{cm}^{-1}\times10^2)$	5.400	5.390	5.278	5.365	5.359
	$C(\mathrm{cm}^{-1}\times10^2)$	3.424	3.467	3.315	3.499	3.411
	κ	–0.334	–0.385	–0.299	–0.384	–0.348
	$\Delta I(\mathrm{amu}\cdot\mathrm{Å}^2)$	0	0	0	–8.76	0
M06-2X/apVTZ & TD-M06-2X /apVTZ	$A(\mathrm{cm}^{-1}\times10^2)$	9.392	9.777	8.931	9.640	9.419
	$B(\mathrm{cm}^{-1}\times10^2)$	5.435	5.425	5.333	5.411	5.399
	$C(\mathrm{cm}^{-1}\times10^2)$	3.443	3.489	3.339	3.555	3.432
	κ	–0.330	–0.384	–0.287	–0.390	–0.343
	$\Delta I(\mathrm{amu}\cdot\mathrm{Å}^2)$	0	0	0	–12.17	0
ωB97X/apVTZ & TD-ωB97X /apVTZ	$A(\mathrm{cm}^{-1}\times10^2)$	9.242	9.772	8.953	9.586	9.426
	$B(\mathrm{cm}^{-1}\times10^2)$	5.442	5.429	5.341	5.409	5.398
	$C(\mathrm{cm}^{-1}\times10^2)$	3.425	3.490	3.345	3.524	3.432
	κ	–0.307	–0.383	–0.288	–0.378	–0.344
	$\Delta I(\mathrm{amu}\cdot\mathrm{Å}^2)$	0	0	0	–9.12	0
MP2/apVDZ & CIS(D)/apVDZ	$A(\mathrm{cm}^{-1}\times10^2)$	9.388	9.754	8.694	9.421	9.236
	$B(\mathrm{cm}^{-1}\times10^2)$	5.387	5.376	5.192	5.275	5.251
	$C(\mathrm{cm}^{-1}\times10^2)$	3.423	3.466	3.251	3.466	3.348
	κ	–0.342	–0.392	–0.287	–0.392	–0.354
	$\Delta I(\mathrm{amu}\cdot\mathrm{Å}^2)$	0	0	0	–12.10	0

Table S3: Predicted Geometries for the $\tilde{X}\,^1\mathrm{A}_1$ Ground State of HFF.

Cartesian coordinates (in Å) are tabulated for the planar equilibrium (C_s) and planar transition-state (C_{2v}) configurations supported by the $\tilde{X}\,^1\mathrm{A}_1$ potential-energy surface of HFF, as optimized by exploiting a variety of quantum-chemical methods in conjunction with augmented correlation-consistent basis sets of double-ζ or triple-ζ quality (where aug-cc-pVDZ ≡ apVDZ and aug-cc-pVTZ ≡ apVTZ). The stationary nature of the resulting geometries was confirmed by the absence or presence of a lone imaginary vibrational frequency in the harmonic force field computed for the minimum-energy or transition-state structures.

		Equilibrium (C_s)			Transition State (C_{2v})		
		x(Å)	y(Å)	z(Å)	x(Å)	y(Å)	z(Å)
HF/apVTZ	C	-0.19097	-1.83880	0.00000	-0.16883	-1.75717	0.00000
	C	0.53065	-0.58977	0.00000	0.54510	-0.56015	0.00000
	C	-1.26942	1.22499	0.00000	-1.34647	1.14156	0.00000
	C	0.00000	0.77057	0.00000	0.00000	0.78160	0.00000
	H	0.43236	-2.73328	0.00000	0.38963	-2.68336	0.00000
	H	-1.44473	2.28510	0.00000	-1.59219	2.19481	0.00000
	C	1.88564	-0.49493	0.00000	1.93504	-0.43100	0.00000
	H	2.56241	-1.32657	0.00000	2.63098	-1.24617	0.00000
	C	2.27418	0.88772	0.00000	2.26643	0.92076	0.00000
	H	3.28174	1.24699	0.00000	3.25736	1.32334	0.00000
	C	1.15122	1.63900	0.00000	1.08619	1.65841	0.00000
	H	1.10269	2.70925	0.00000	1.01644	2.72797	0.00000
	H	-2.18862	-0.41298	0.00000	-1.93127	-0.78460	0.00000
	O	-2.36669	0.53370	0.00000	-2.30071	0.34426	0.00000
	O	-1.38752	-1.95384	0.00000	-1.40876	-1.85127	0.00000
B3LYP/apVTZ	C	-0.19097	-1.83880	0.00000	1.57614	-0.81261	0.00000
	C	0.53065	-0.58977	0.00000	0.72924	0.29555	0.00000
	C	-1.26942	1.22499	0.00000	-1.57614	-0.81261	0.00000
	C	0.00000	0.77057	0.00000	-0.72924	0.29555	0.00000
	H	0.43236	-2.73328	0.00000	2.65380	-0.63769	0.00000
	H	-1.44473	2.28510	0.00000	-2.65380	-0.63769	0.00000
	C	1.88564	-0.49493	0.00000	1.13557	1.64515	0.00000
	H	2.56241	-1.32657	0.00000	2.16061	1.98402	0.00000
	C	2.27418	0.88772	0.00000	0.00000	2.46156	0.00000
	H	3.28174	1.24699	0.00000	0.00000	3.53970	0.00000
	C	1.15122	1.63900	0.00000	-1.13557	1.64515	0.00000
	H	1.10269	2.70925	0.00000	-2.16061	1.98402	0.00000
	H	-2.18862	-0.41298	0.00000	0.00000	-2.10235	0.00000
	O	-2.36669	0.53370	0.00000	-1.20562	-2.02728	0.00000
	O	-1.38752	-1.95384	0.00000	1.20562	-2.02728	0.00000
M06-2X/apVTZ	C	-0.17247	-1.80447	0.00000	1.57233	-0.81357	0.00000
	C	0.54304	-0.57248	0.00000	0.72530	0.29542	0.00000
	C	-1.30757	1.18120	0.00000	-1.57233	-0.81357	0.00000
	C	0.00000	0.77610	0.00000	-0.72530	0.29542	0.00000
	H	0.43796	-2.71772	0.00000	2.64993	-0.63724	0.00000
	H	-1.53457	2.24371	0.00000	-2.64993	-0.63724	0.00000
	C	1.92070	-0.45538	0.00000	1.13347	1.63915	0.00000
	H	2.61170	-1.28605	0.00000	2.16051	1.97338	0.00000
	C	2.27451	0.92056	0.00000	0.00000	2.45579	0.00000
	H	3.28022	1.30817	0.00000	0.00000	3.53358	0.00000
	C	1.11886	1.66465	0.00000	-1.13347	1.63915	0.00000
	H	1.04608	2.74195	0.00000	-2.16051	1.97338	0.00000
	H	-2.07239	-0.56801	0.00000	0.00000	-2.09341	0.00000
	O	-2.35359	0.41993	0.00000	-1.20000	-2.01870	0.00000
	O	-1.40033	-1.91782	0.00000	1.20000	-2.01870	0.00000

		Equilibrium (C_s)			Transition State (C_{2v})		
		x(Å)	y(Å)	z(Å)	x(Å)	y(Å)	z(Å)
ωB97X/apVTZ	C	-0.17300	-1.81505	0.00000	-1.34579	-1.14982	0.00000
	C	0.54082	-0.57673	0.00000	0.00000	-0.78327	0.00000
	C	-1.29762	1.19514	0.00000	-0.15900	1.76292	0.00000
	C	0.00000	0.77472	0.00000	0.54741	0.56025	0.00000
	H	0.44651	-2.72499	0.00000	-1.59050	-2.21497	0.00000
	H	-1.51327	2.26024	0.00000	0.41036	2.69579	0.00000
	C	1.91360	-0.46363	0.00000	1.09008	-1.66642	0.00000
	H	2.60359	-1.29667	0.00000	1.01425	-2.74500	0.00000
	C	2.27500	0.91291	0.00000	2.27279	-0.92601	0.00000
	H	3.28400	1.29542	0.00000	3.27209	-1.33317	0.00000
	C	1.12698	1.65880	0.00000	1.94432	0.43006	0.00000
	H	1.06019	2.73763	0.00000	2.64381	1.25456	0.00000
	H	-2.10509	-0.52241	0.00000	-1.93613	0.78895	0.00000
	O	-2.36389	0.45245	0.00000	-1.41608	1.87472	0.00000
	O	-1.39743	-1.93571	0.00000	-2.32302	-0.35127	0.00000
MP2/apVDZ	C	-0.16016	-1.82126	0.00000	-0.15820	1.77867	0.00000
	C	0.55052	-0.57232	0.00000	0.55427	0.55993	0.00000
	C	-1.33125	1.18149	0.00000	-1.36374	-1.15279	0.00000
	C	0.00000	0.77995	0.00000	0.00000	-0.78787	0.00000
	H	0.46306	-2.73842	0.00000	0.41680	2.71905	0.00000
	H	-1.57149	2.25191	0.00000	-1.61665	-2.22562	0.00000
	C	1.95544	-0.44515	0.00000	1.97524	0.43181	0.00000
	H	2.66038	-1.28085	0.00000	2.68260	1.26495	0.00000
	C	2.29729	0.94537	0.00000	2.29955	-0.94567	0.00000
	H	3.31130	1.34924	0.00000	3.30908	-1.36083	0.00000
	C	1.11641	1.69603	0.00000	1.10000	-1.69648	0.00000
	H	1.03370	2.78549	0.00000	1.01659	-2.78621	0.00000
	H	-2.07877	-0.57803	0.00000	-1.94163	0.79849	0.00000
	O	-2.38795	0.40350	0.00000	-2.35355	-0.33760	0.00000
	O	-1.41051	-1.95025	0.00000	-1.43514	1.89567	0.00000
MP2/apVTZ	C	-0.15875	-1.80300	0.00000	-0.81419	1.57213	0.00000
	C	0.54601	-0.56670	0.00000	0.29703	0.72276	0.00000
	C	-1.31964	1.17038	0.00000	-0.81419	-1.57213	0.00000
	C	0.00000	0.77421	0.00000	0.29703	-0.72276	0.00000
	H	0.45828	-2.71137	0.00000	-0.63736	2.64948	0.00000
	H	-1.55533	2.23109	0.00000	-0.63736	-2.64948	0.00000
	C	1.93799	-0.44049	0.00000	1.64760	1.13943	0.00000
	H	2.63424	-1.26817	0.00000	1.98032	2.16816	0.00000
	C	2.27654	0.93660	0.00000	2.46378	0.00000	0.00000
	H	3.27929	1.33592	0.00000	3.54316	0.00000	0.00000
	C	1.10688	1.68020	0.00000	1.64760	-1.13943	0.00000
	H	1.02442	2.75791	0.00000	1.98032	-2.16816	0.00000
	H	-2.05572	-0.58573	0.00000	-2.08534	0.00000	0.00000
	O	-2.36525	0.39814	0.00000	-2.03073	-1.20161	0.00000
	O	-1.39967	-1.93150	0.00000	-2.03073	1.20161	0.00000

		Equilibrium (C_s)			Transition State (C_{2v})		
		x(Å)	y(Å)	z(Å)	x(Å)	y(Å)	z(Å)
MP3/apVDZ	C	-0.18165	-1.84359	0.00000	-0.82674	-1.58308	0.00000
	C	0.54292	-0.58516	0.00000	0.29798	-0.73135	0.00000
	C	-1.30619	1.21403	0.00000	-0.82674	1.58308	0.00000
	C	0.00000	0.78244	0.00000	0.29798	0.73135	0.00000
	H	0.44626	-2.75753	0.00000	-0.65592	-2.67060	0.00000
	H	-1.51822	2.28791	0.00000	-0.65592	2.67060	0.00000
	C	1.93121	-0.48039	0.00000	1.65855	-1.14915	0.00000
	H	2.62542	-1.32226	0.00000	1.99864	-2.18543	0.00000
	C	2.30499	0.92088	0.00000	2.48452	0.00000	0.00000
	H	3.32622	1.29980	0.00000	3.57369	0.00000	0.00000
	C	1.14867	1.68127	0.00000	1.65855	1.14915	0.00000
	H	1.08428	2.76974	0.00000	1.99863	2.18543	0.00000
	H	-2.14270	-0.49220	0.00000	-2.09829	0.00000	0.00000
	O	-2.39740	0.47064	0.00000	-2.03909	1.19983	0.00000
	O	-1.41022	-1.96093	0.00000	-2.03909	-1.19983	0.00000
CCSD/apVDZ	C	-0.17756	-1.84529	0.00000	-0.82447	1.58560	0.00000
	C	0.54503	-0.58536	0.00000	0.29914	0.73187	0.00000
	C	-1.30621	1.21574	0.00000	-0.82447	-1.58560	0.00000
	C	0.00000	0.78216	0.00000	0.29914	-0.73186	0.00000
	H	0.45257	-2.75981	0.00000	-0.65346	2.67464	0.00000
	H	-1.51909	2.29101	0.00000	-0.65346	-2.67464	0.00000
	C	1.93286	-0.47841	0.00000	1.65927	1.14853	0.00000
	H	2.62921	-1.32132	0.00000	1.99980	2.18701	0.00000
	C	2.30640	0.92361	0.00000	2.48689	0.00000	0.00000
	H	3.32900	1.30452	0.00000	3.57808	0.00000	0.00000
	C	1.14802	1.68137	0.00000	1.65927	-1.14853	0.00000
	H	1.08220	2.77184	0.00000	1.99980	-2.18700	0.00000
	H	-2.14576	-0.49254	0.00000	-2.10091	-0.00001	0.00000
	O	-2.40288	0.47246	0.00000	-2.04366	-1.20360	0.00000
	O	-1.41204	-1.96702	0.00000	-2.04366	1.20360	0.00000
CCSD(T)/apVDZ	C	0.00000	0.00000	0.00000	0.00000	0.00000	0.00000
	C	0.00000	1.44839	0.00000	0.00000	1.20938	0.00000
	C	2.51150	2.07198	0.00000	0.10621	-1.20471	0.00000
	C	1.15641	2.36129	0.00000	1.20963	1.64548	0.00000
	H	-1.00120	-0.48485	0.00000	1.34946	-1.53289	0.00000
	H	3.24228	2.89233	0.00000	1.33334	2.74311	0.00000
	C	-1.15700	2.24449	0.00000	1.56909	-2.61541	0.00000
	H	-2.18401	1.86309	0.00000	2.37097	0.83901	0.00000
	C	-0.77498	3.64188	0.00000	2.43550	-0.62755	0.00000
	H	-1.46737	4.48818	0.00000	3.71780	1.31776	0.00000
	C	0.61831	3.71600	0.00000	3.81917	-0.98616	0.00000
	H	1.22421	4.62774	0.00000	4.01212	2.37257	0.00000
	H	2.34598	0.16837	0.00000	4.20498	-2.01104	0.00000
	O	3.07364	0.87086	0.00000	4.59771	0.20228	0.00000
	O	1.01966	-0.72669	0.00000	5.69011	0.25034	0.00000

Table S4: Predicted Geometries for the $\tilde{A}^1B_2$ Excited State of HFF.

Cartesian coordinates (in Å) are tabulated for the planar equilibrium (C_s), aplanar transition-state (C_2), and planar second-order saddle-point (C_{2v}) configurations supported by the $\tilde{A}^1B_2\left(\pi^*\pi\right)$ potential-energy surface of HFF as optimized by exploiting a variety of quantum-chemical methods in conjunction with augmented correlation-consistent basis sets of double-ζ or triple-ζ quality (where aug-cc-pVDZ ≡ apVDZ and aug-cc-pVTZ ≡ apVTZ). The stationary nature of the resulting geometries was confirmed by the presence of zero, one, or two imaginary vibrational frequencies in the harmonic force field computed for the minimum-energy, transition-state, or saddle-point structures, respectively.

		Equilibrium (C_s)			Transition State (C_2)			2nd Order Saddle Point (C_{2v})		
		x(Å)	y(Å)	z(Å)	x(Å)	y(Å)	z(Å)	x(Å)	y(Å)	z(Å)
CIS/apVTZ	C	0.69567	1.70402	0.00000	0.82772	1.58321	0.00380	-0.82130	-1.59458	0.00000
	C	-0.34685	0.70377	0.00000	-0.30055	0.75694	-0.06573	0.30399	-0.76149	0.00000
	C	0.88689	-1.58193	0.00000	0.82772	-1.58321	-0.00380	-0.82130	1.59458	0.00000
	C	-0.21315	-0.75686	0.00000	-0.30055	-0.75694	0.06573	0.30399	0.76149	0.00000
	H	0.34347	2.73558	0.00000	0.69235	2.64791	-0.11197	-0.66176	-2.66216	0.00000
	H	0.74101	-2.64241	0.00000	0.69235	-2.64791	0.11197	-0.66176	2.66216	0.00000
	C	-1.74229	1.04373	0.00000	-1.63051	1.14767	-0.14823	1.63587	-1.15655	0.00000
	H	-2.13152	2.03936	0.00000	-1.98803	2.15063	-0.24599	1.99305	-2.16437	0.00000
	C	-2.45217	-0.11572	0.00000	-2.43572	0.00000	0.00000	2.44187	0.00000	0.00000
	H	-3.51703	-0.21711	0.00000	-3.50640	0.00000	0.00000	3.51248	0.00000	0.00000
	C	-1.52617	-1.22455	0.00000	-1.63051	-1.14767	0.14823	1.63587	1.15655	0.00000
	H	-1.81438	-2.25646	0.00000	-1.98803	-2.15063	0.24599	1.99305	2.16437	0.00000
	H	2.26277	-0.28195	0.00000	2.07984	0.00000	0.00000	-2.08221	0.00000	0.00000
	O	2.16080	-1.22969	0.00000	1.99202	-1.16458	-0.22634	-2.01043	1.18974	0.00000
	O	1.87722	1.47822	0.00000	1.99202	1.16458	0.22634	-2.01043	-1.18974	0.00000
CIS(D)/apVDZ	C	0.00000	0.00000	0.00000	0.00000	0.00000	0.00000	0.00000	0.00000	0.00000
	C	0.00000	1.42562	0.00000	0.00000	0.00000	1.20796	0.00000	1.21767	0.00000
	C	2.61979	2.08897	0.00000	0.15279	0.00000	-1.19826	0.06924	-1.21570	0.00000
	C	1.16250	2.34670	0.00000	1.14370	-0.48872	1.59212	1.22245	1.65842	0.00000
	H	-0.99549	-0.48929	0.00000	1.33590	0.48872	-1.43467	1.31477	-1.58623	0.00000
	H	3.32403	2.92343	0.00000	1.18539	-0.98903	2.57063	1.35972	2.74941	0.00000
	C	-1.24319	2.24558	0.00000	1.50103	0.98903	-2.40004	1.51386	-2.66764	0.00000
	H	-2.25348	1.83475	0.00000	2.34142	-0.32863	0.83011	2.38334	0.82582	0.00000
	C	-0.87458	3.54932	0.00000	2.42762	0.32863	-0.52728	2.42644	-0.68897	0.00000
	H	-1.51988	4.42942	0.00000	3.66099	-0.56518	1.27197	3.71791	1.28699	0.00000
	C	0.65588	3.60333	0.00000	3.79248	0.56518	-0.79868	3.78507	-1.07350	0.00000
	H	1.23951	4.52815	0.00000	3.95290	-1.00611	2.22609	4.03872	2.32944	0.00000
	H	2.43137	0.18010	0.00000	4.20273	1.00611	-1.70821	4.16464	-2.09602	0.00000
	O	3.16697	0.85347	0.00000	4.55335	0.00000	0.28914	4.58272	0.13040	0.00000
	O	1.02511	-0.73100	0.00000	5.64347	0.00000	0.35836	5.67445	0.16146	0.00000

		Equilibrium (C_s)			Transition State (C_2)			2nd Order Saddle Point (C_{2v})		
		x(Å)	y(Å)	z(Å)	x(Å)	y(Å)	z(Å)	x(Å)	y(Å)	z(Å)
TD-B3LYP/apVTZ	C	-0.64786	1.69319	0.00000	0.83275	-1.58498	-0.00771	1.61067	-0.81698	0.00000
	C	0.36367	0.67891	0.00000	-0.30438	-0.74627	-0.08169	0.75191	0.30865	0.00000
	C	-0.96382	-1.59427	0.00000	0.83275	1.58498	0.00771	-1.61067	-0.81698	0.00000
	C	0.21759	-0.75293	0.00000	-0.30438	0.74627	0.08169	-0.75191	0.30865	0.00000
	H	-0.28161	2.73099	0.00000	0.72038	-2.64997	-0.20540	2.68610	-0.64664	0.00000
	H	-0.87084	-2.66756	0.00000	0.72038	2.64997	0.20539	-2.68610	-0.64664	0.00000
	C	1.80487	1.01023	0.00000	-1.63821	-1.14685	-0.18470	1.16111	1.64458	0.00000
	H	2.19894	2.01350	0.00000	-1.98898	-2.15830	-0.30871	2.18052	1.99391	0.00000
	C	2.48782	-0.14566	0.00000	-2.45657	0.00000	0.00000	0.00000	2.46574	0.00000
	H	3.55653	-0.28367	0.00000	-3.53556	0.00000	0.00000	0.00000	3.54461	0.00000
	C	1.49506	-1.24597	0.00000	-1.63821	1.14685	0.18470	-1.16111	1.64458	0.00000
	H	1.75657	-2.29537	0.00000	-1.98898	2.15830	0.30871	-2.18052	1.99391	0.00000
	H	-2.22641	-0.15339	0.00000	2.10261	0.00000	0.00000	0.00000	-2.09662	0.00000
	O	-2.21781	-1.14319	0.00000	2.00173	1.16244	-0.31406	-1.21662	-2.03575	0.00000
	O	-1.86684	1.49252	0.00000	2.00173	-1.16244	0.31406	1.21662	-2.03575	0.00000
TD-M06-2X/apVTZ	C	0.66712	1.69113	0.00000	0.83706	-1.57333	-0.00209	1.60672	-0.81642	0.00000
	C	-0.35974	0.68461	0.00000	-0.29993	-0.74596	-0.10062	0.75640	0.30719	0.00000
	C	0.93512	-1.58766	0.00000	0.83706	1.57333	0.00209	-1.60672	-0.81642	0.00000
	C	-0.21765	-0.75190	0.00000	-0.29993	0.74596	0.10062	-0.75640	0.30719	0.00000
	H	0.30978	2.73160	0.00000	0.73988	-2.63756	-0.21276	2.68256	-0.64597	0.00000
	H	0.82194	-2.66061	0.00000	0.73988	2.63756	0.21276	-2.68256	-0.64597	0.00000
	C	-1.78432	1.02422	0.00000	-1.62966	-1.14024	-0.22286	1.16105	1.64000	0.00000
	H	-2.17425	2.02916	0.00000	-1.98101	-2.14866	-0.36938	2.18048	1.98990	0.00000
	C	-2.47540	-0.13222	0.00000	-2.44197	0.00000	0.00000	0.00000	2.45484	0.00000
	H	-3.54579	-0.25908	0.00000	-3.52143	0.00000	0.00000	0.00000	3.53421	0.00000
	C	-1.50067	-1.23888	0.00000	-1.62967	1.14024	0.22286	-1.16105	1.64000	0.00000
	H	-1.76574	-2.28714	0.00000	-1.98101	2.14866	0.36938	-2.18048	1.98990	0.00000
	H	2.22263	-0.17841	0.00000	2.09277	0.00000	0.00000	0.00000	-2.08776	0.00000
	O	2.19468	-1.16308	0.00000	1.97957	1.13825	-0.36785	-1.21004	-2.02704	0.00000
	O	1.87341	1.47417	0.00000	1.97957	-1.13825	0.36785	1.21004	-2.02704	0.00000

		Equilibrium (C_s)			Transition State (C_2)			2nd Order Saddle Point (C_{2v})		
		x(Å)	y(Å)	z(Å)	x(Å)	y(Å)	z(Å)	x(Å)	y(Å)	z(Å)
TD-ωB97X/apVTZ	C	0.67801	1.68577	0.00000	0.82956	1.58087	0.00136	-1.37316	1.18987	0.00000
	C	-0.35453	0.69043	0.00000	-0.30061	0.74917	0.08809	0.00000	0.77593	0.00000
	C	0.91873	-1.58242	0.00000	0.82956	-1.58087	-0.00108	-0.09441	-1.82743	0.00000
	C	-0.22174	-0.75077	0.00000	-0.30058	-0.74917	-0.08819	0.54029	-0.56669	0.00000
	H	0.32951	2.73065	0.00000	0.71294	2.65048	0.17763	-1.54021	2.27860	0.00000
	H	0.79955	-2.65622	0.00000	0.71300	-2.65048	-0.17739	0.50198	-2.72829	0.00000
	C	-1.77711	1.03242	0.00000	-1.63316	1.14345	0.19636	1.10915	1.73009	0.00000
	H	-2.16798	2.03807	0.00000	-1.98687	2.15436	0.32595	0.99737	2.80323	0.00000
	C	-2.47119	-0.12261	0.00000	-2.44238	0.00000	-0.00041	2.25429	1.01983	0.00000
	H	-3.54371	-0.24208	0.00000	-3.52284	0.00000	-0.00059	3.26292	1.40353	0.00000
	C	-1.50886	-1.23321	0.00000	-1.63310	-1.14345	-0.19691	1.90568	-0.40778	0.00000
	H	-1.78109	-2.28033	0.00000	-1.98676	-2.15436	-0.32661	2.62618	-1.21491	0.00000
	H	2.22131	-0.19251	0.00000	2.08761	0.00000	0.00035	-1.88795	-1.18571	0.00000
	O	2.18388	-1.17610	0.00000	1.99290	-1.15827	0.31651	-1.40549	-2.04366	0.00000
	O	1.88644	1.46170	0.00000	1.99300	1.15827	-0.31585	-2.34592	0.43873	0.00000
EOM-CCSD/apVDZ	C	-0.16363	-1.83349	0.00000	-0.84650	-1.57313	-0.25264	0.82730	1.62130	0.00000
	C	0.55770	-0.58310	0.00000	0.30536	-0.73983	-0.17531	-0.30991	0.76411	0.00000
	C	-1.35750	1.27369	0.00000	-0.83775	1.59124	0.14578	0.82730	-1.62130	0.00000
	C	0.00000	0.78527	0.00000	0.29653	0.73336	0.21349	-0.30991	-0.76411	0.00000
	H	0.46163	-2.75092	0.00000	-0.73300	-2.62440	-0.55685	0.66284	2.70906	0.00000
	H	-1.55179	2.34819	0.00000	-0.74110	2.64025	0.46332	0.66284	-2.70906	0.00000
	C	2.02470	-0.48842	0.00000	1.65775	-1.13958	-0.25296	-1.66135	1.17655	0.00000
	H	2.70668	-1.33960	0.00000	2.01869	-2.13998	-0.49652	-2.01526	2.20851	0.00000
	C	2.35804	0.84495	0.00000	2.47313	-0.02660	0.15692	-2.49176	0.00000	0.00000
	H	3.35874	1.28022	0.00000	3.56323	-0.03832	0.22608	-3.58398	0.00000	0.00000
	C	1.08940	1.63507	0.00000	1.63653	1.10415	0.46197	-1.66135	-1.17655	0.00000
	H	1.03725	2.72749	0.00000	1.98513	2.09692	0.75055	-2.01526	-2.20851	0.00000
	H	-2.18130	-0.45293	0.00000	-2.08814	0.02246	-0.13249	2.09743	0.00000	0.00000
	O	-2.45449	0.50072	0.00000	-1.98179	1.20764	-0.32666	2.05434	-1.21336	0.00000
	O	-1.40594	-1.95275	0.00000	-2.03260	-1.16447	0.07195	2.05434	1.21336	0.00000

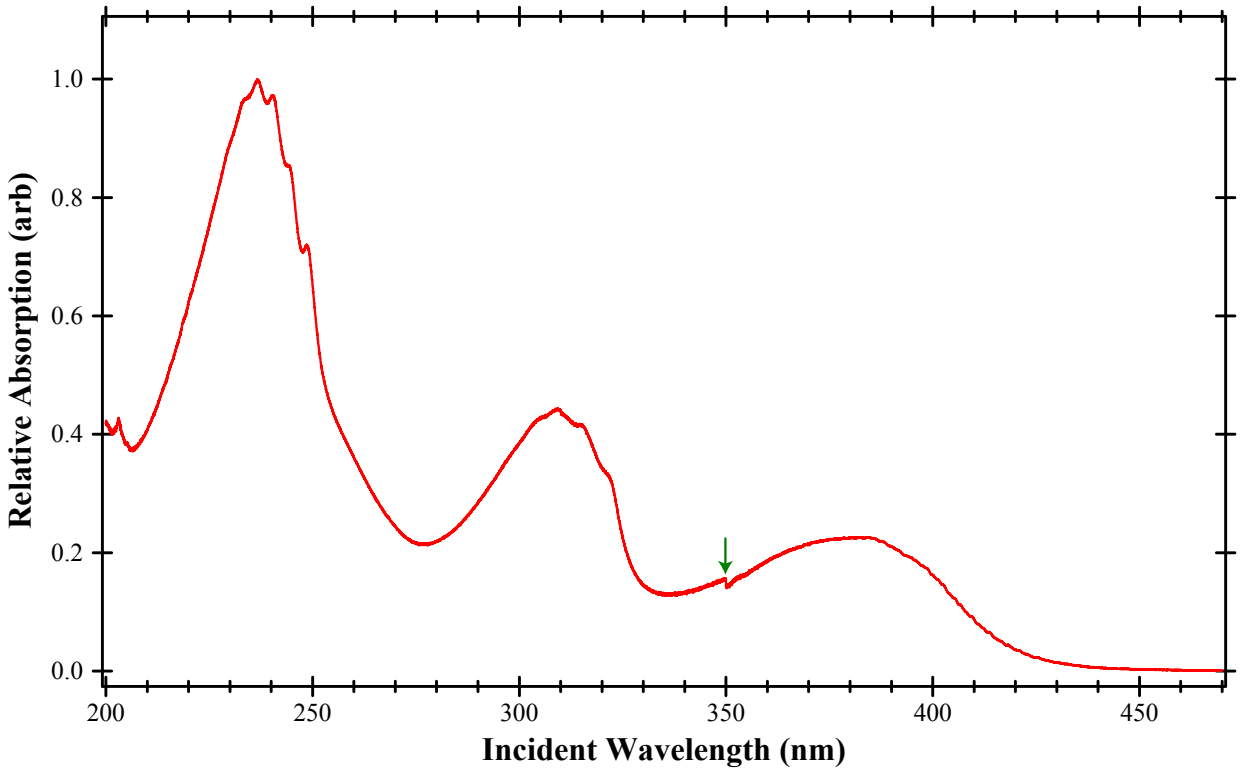

Figure S1: Broadband UV-VIS Spectrum of HFF Electronic States.

The UV-VIS spectrum of ambient ($25^{\circ}\mathrm{C}$) gas-phase HFF is presented over an incident range of wavelengths extending from $470\,\mathrm{nm}$ to $200\,\mathrm{nm}$. Three strong absorption systems of monotonically increasing intensity are found, with the extracted λ_{max} values of 381.88, 309.32, and $236.60\,\mathrm{nm}$ in reasonable accord with previous datasets acquired for HFF in dilute solutions (see text for details). The spurious dip in the spectral trace at $\sim 350\,\mathrm{nm}$ (*cf.* superimposed arrow) reflects an instrumental artifact arising from changeover of the excitation source.

Figure S2: Source of Isotopic Shift for the $\tilde{A}-\tilde{X}$ Origin Band.

The various contributions to the location of the origin band in the $\tilde{A}\,^1\mathrm{B}_2-\tilde{X}\,^1\mathrm{A}_1$ $\left(\pi^*\leftarrow\pi\right)$ absorption system are depicted schematically for HFF (on the left) and HFF-*d* (on the right). The spectral shift of this feature upon isotopic substitution, $\delta\nu_{00}$, reflects the relative changes in zero-point energies (ZPEs) between the ground and excited states ($\delta_{ZPE}^{\tilde{A}}-\delta_{ZPE}^{\tilde{X}}$) as well as the associated differences in state-specific tunneling metrics, $(d_{\mathrm{H}}^{\tilde{X}}-d_{\mathrm{D}}^{\tilde{X}})+(d_{\mathrm{H}}^{\tilde{A}}-d_{\mathrm{D}}^{\tilde{A}})$, where $d_i^{\eta}=\Delta_i^{\eta}/2$ defines the equal magnitude of the energy displacement experienced by the two parity components (*e.g.*, $0_+/0_-$ in the ground state and $0^+/0^-$ in the excited state) of the vibrationless ($\mathrm{v}=0$) tunneling doublet for isotopolog $i=\mathrm{H}$ or D in electronic manifold $\eta=\tilde{X}$ or $\tilde{A}$. While the pronounced quenching of unimolecular dynamics in the $\tilde{A}\,^1\mathrm{B}_2$ state imparts negligible effects for $\delta\nu_{00}$, the enormous tunneling-induced bifurcation of the vibrationless $\tilde{X}\,^1\mathrm{A}_1$ level (presumed to split symmetrically about the hypothetical tunneling-free ZPE denoted by a dashed green line) produces a sizable offset of $d_{\mathrm{H}}^{\tilde{X}}-d_{\mathrm{D}}^{\tilde{X}}=44\,\mathrm{cm}^{-1}$ that represents a significant fraction of the experimentally observed spectral shift.

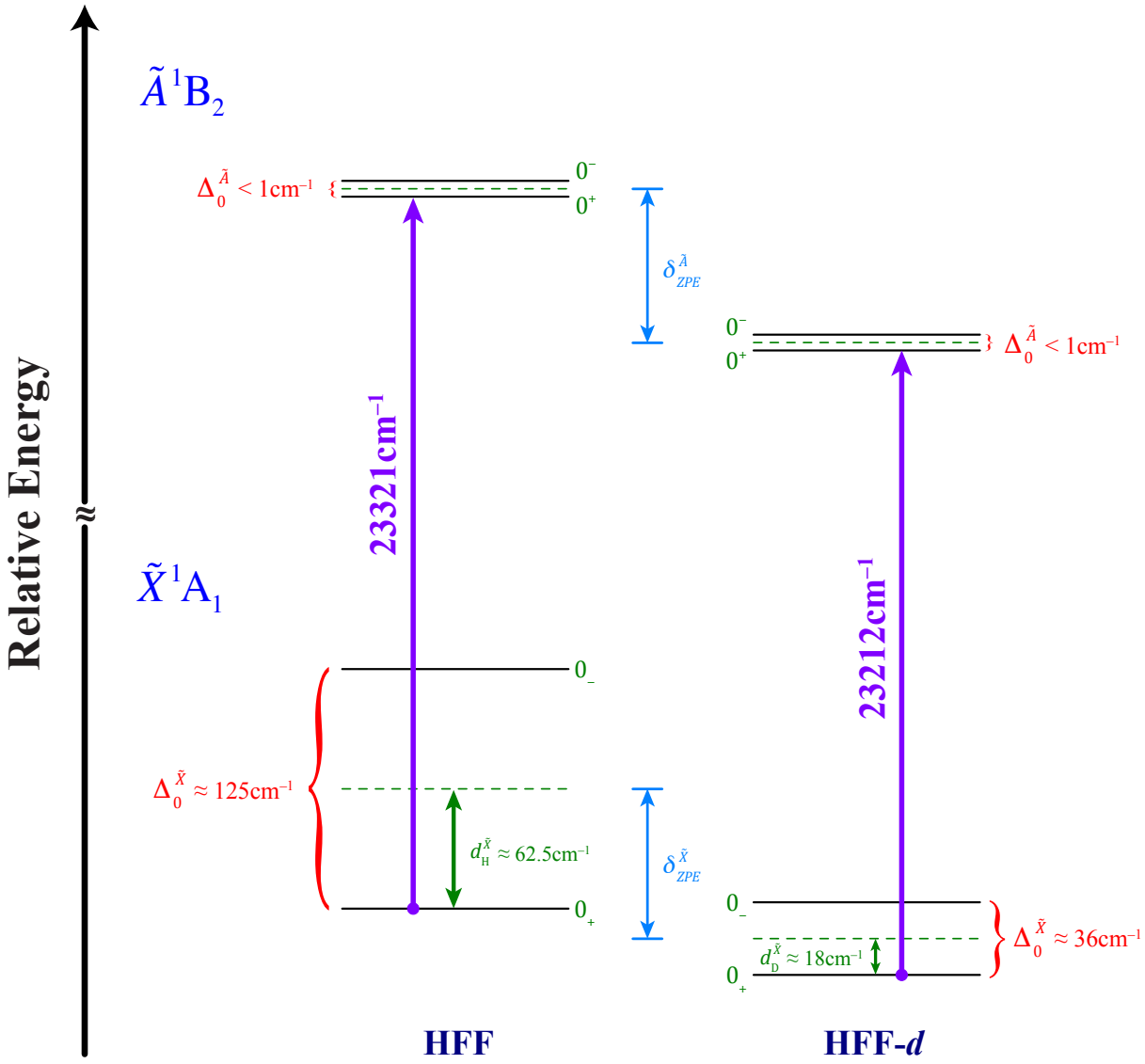
Relative Energy
$\tilde{A}\,^1B_2$
$\tilde{X}\,^1A_1$
$\Delta_0^{\tilde{A}} < 1\text{cm}^{-1}$
0^-
0^+
$\delta_{ZPE}^{\tilde{A}}$
23321cm^{-1}
0_-
$\Delta_0^{\tilde{X}} \approx 125\text{cm}^{-1}$
$d_H^{\tilde{X}} \approx 62.5\text{cm}^{-1}$
0_+
$\delta_{ZPE}^{\tilde{X}}$
HFF
0^-
0^+
$\Delta_0^{\tilde{A}} < 1\text{cm}^{-1}$
23212cm^{-1}
0_-
$d_D^{\tilde{X}} \approx 18\text{cm}^{-1}$
0_+
$\Delta_0^{\tilde{X}} \approx 36\text{cm}^{-1}$
HFF-*d*

Figure S3: Allowed Vibronic Transitions in Jet-Cooled HFF.

A schematic energy level diagram is presented for absorption processes originating from the vibrationless (zero-point) level in $\tilde{X}\,^1\mathrm{A}_1$ HFF and terminating on an $\tilde{A}\,^1\mathrm{B}_2$ vibronic level having either a_1 (left diagram) or b_2 (right diagram) vibrational parentage. Solid (dotted) lines reflect strongly (weakly) allowed transitions arising from the *b*-polarized (*a*-polarized) component of the transition dipole moment, with resonances starting from the symmetric (0_+) or antisymmetric (0_-) ground-state tunneling component distinguished by blue and purple colors, respectively. The total symmetry (Γ_{tot}) for each vibronic-tunneling state (as classified through irreducible representations of the encompassing G_4 molecular-symmetry group) follows from the direct product of electronic (Γ_e), vibrational (Γ_v), and tunneling (Γ_t) contributions. Given the $\Gamma^{\mathrm{TDM}} = a_1$ (type-*b*) or $\Gamma^{\mathrm{TDM}} = b_2$ (type-*a*) nature of the transition dipole moment for the HFF $\pi^* \leftarrow \pi$ system, transitions between ground-state ($\Gamma_{tot} \equiv \Gamma_0^{\tilde{X}}$) and excited-state ($\Gamma_{tot} \equiv \Gamma_v^{\tilde{A}}$) levels are allowed only when the $\Gamma_0^{\tilde{X}} \otimes \Gamma^{\mathrm{TDM}} \otimes \Gamma_v^{\tilde{A}}$ direct product includes the totally-symmetric representation (*viz.*, when $\Gamma_0^{\tilde{X}} \otimes \Gamma^{\mathrm{TDM}} \otimes \Gamma_v^{\tilde{A}} = a_1$).

Transitions to a_1 Vibrations in the Excited State

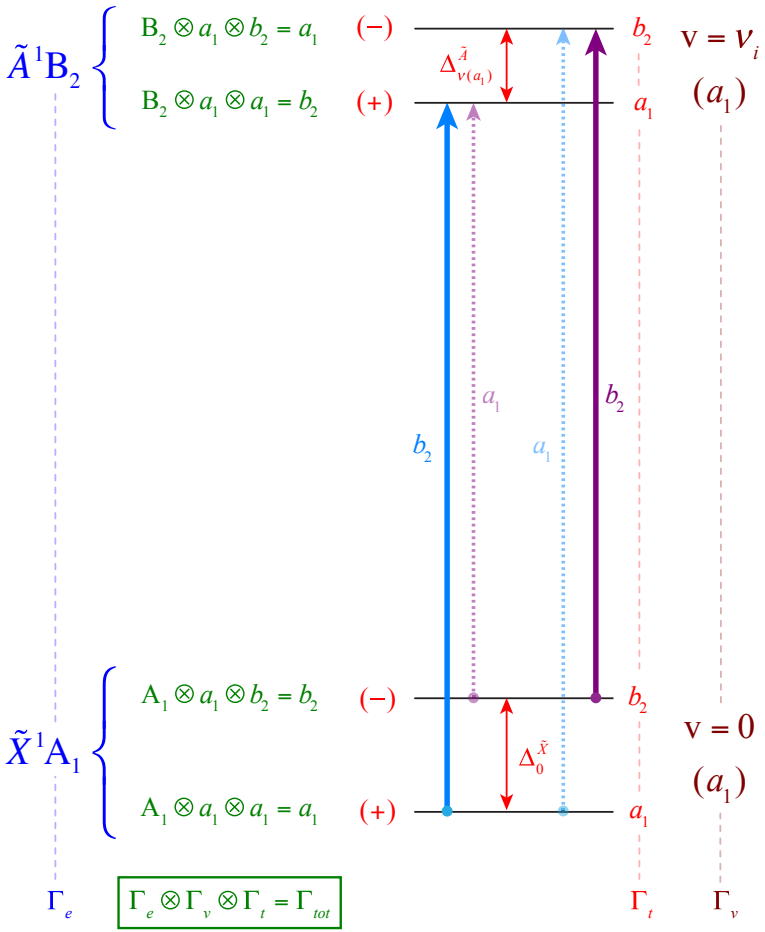

Transitions to b_2 Vibrations in the Excited State